Architecture of a Biocompatible Supramolecular Material by Supersaturation-Driven Fabrication of its Fiber Network

Jing-Liang Li, Xiang-Yang Liu,* Rong-Yao Wang, and Jun-Ying Xiong

Department of Physics, National University of Singapore, 2 Science Drive 3, Singapore 117542

Received: August 18, 2005; In Final Form: October 26, 2005

The architecture of a biocompatible organogel formed by gelation of a small molecule organic gelator, *N*-lauroyl-L-glutamic acid di-*n*-butylamide, in isostearyl alcohol was investigated based on a supersaturation-driven crystallographic mismatch branching mechanism. By controlling the supersaturation of the system, the correlation length that determines the mesh size of the fiber network was finely tuned and the rheological properties of the gel were engineered. This approach is of considerable significance for many gel-based applications, such as controlled release of drugs that requires precise control of the mesh size. A direct cryo-transmission electron microscopy (TEM) imaging technique capable of preserving the network structure was used to visualize its nanostructure.

I. Introduction

Organogel formed by the gelation of a small molecule organic gelator in organic solvents is a class of supramolecular materials that has attracted significant research interest in recent years.[1−5] In such a system, the molecules of the gelator self-organize into a three-dimensional fibrous network that effectively entraps the solvent through capillary force or surface tension. In view of the three-dimensional (3D) fibrous network structures and the solvent-trapping capacity, these materials have important applications in drug delivery,[6−8] as templates for the fabrication of nanostructures,[9−11] as scaffolds for tissue engineering and self-supporting porous materials for the separation of macromolecules, and so forth.[12,13] In general, the fiber network structure of this type of materials determines their performance and even applicability. For instance, an effective drug delivery and bioseparation process depends on the precise control of the mesh size of the network. Therefore, for a given system, it is very desirable to be able to manipulate the formation of the network, so as to obtain the preferred fiber network structure.

It is generally believed that the fiber network of supramolecular materials is formed by molecular self-assembly through highly specific noncovalent interactions.[1,14] Interestingly, recent research confirmed that for many gel systems the network formation is a nucleation−growth process that consists of the primary nucleation of the gelators and the subsequent growth of the fibers.[4,15,16] According to this mechanism, the entire network of a gel is composed of a number of individual smaller fiber networks (structure unit), each of which originated from a primary nucleation site. The fibers of one structure unit entangle with those of other structure units to form the entire network. On the basis of this nucleation−growth mechanism, a permanent and strong 3D fiber network can only be formed when branching occurs at the tips or the side faces of growing fibers. This is called "crystallographic mismatch branching" (CMB) (Figure 1). CMB occurs when the new layers on the tips of the growing fibrils undergo a certain degree of structural mismatch. The structural match can be controlled by changing the supersaturation of the gelator or using suitable additives to influence the correlation between the fiber tips and the nucleating phase.[17]

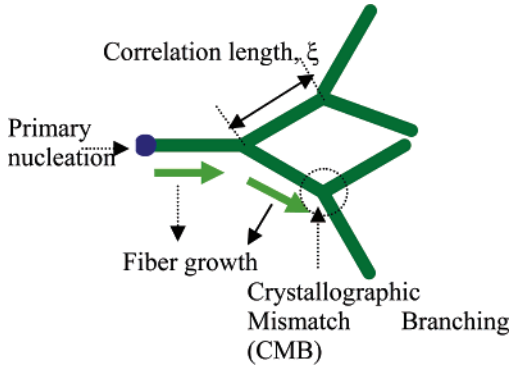

Figure 1. Formation of a fiber network based on the nucleation−growth mechanism. Fiber branching can be caused by high surface supersaturation (supersaturation-driven CMB) on the fiber tips or by the adsorption of additives (additive-induced CMB).

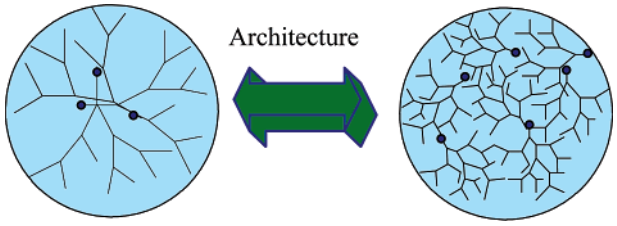

Figure 2. Architecture of the gel network. Individual networks originating from primary nucleation sites ultimately form the entire network. The number of individual networks, the correlation length, the mesh size, and the material properties can be finely tuned by controlling the supersaturation.

The nucleation−growth mechanism of the gel network formation implies that it is feasible to control the fiber growth, so as to obtain materials with the desired fiber network (Figure 2). The fiber network structure also determines the macroscopic properties of a gel such as its hardness and elasticity. In this paper, a biocompatible gel, which is formed by the gelation of isostearyl alcohol by a small molecule organic gelator, *N*-

* Author for correspondence. Tel.: +65-68742812. Fax: +65-67776126. E-mail: phyliuxy@nus.edu.sg.

10.1021/jp054676y CCC: $30.25
Published on Web 12/06/2005

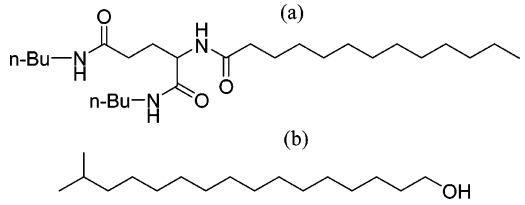

Figure 3. Molecular structure of *N*-lauroyl-L-glutamic acid di-*n*-butylamide (a) and isostearyl alcohol (b).

lauroyl-L-glutamic acid di-*n*-butylamide, is used a model. The architecture of its fiber network is investigated, and the influence of network structure on the rheological properties of the gel is also studied. Isostearyl alcohol is a long chain fatty alcohol that has been found to be biocompatible with skin and is being used in skin care products.[8,18,19] Therefore, influencing the architecture of this type of biocompatible material is an important step toward the formation of pharmaceutical products of high performance.

II. Materials and Methods

II.A. Materials. The gelator, *N*-lauroyl-L-glutamic acid di-*n*-butylamide (GP-1), and the solvent, isostearyl alcohol (ISA), were both obtained from Kishimoto Sangyo Asia. The GP-1 used was in a crystalline powder state. Except in the dissolution experiments, the GP-1 concentration was fixed at 4.93 mol %. Different supersaturations were obtained by controlling the gelation temperature. The molecular structures of GP-1 and ISA are given in Figure 3.

II.B. Measurement of GP-1 Solubility in ISA. Gels at a series of concentrations, $X°$, were prepared in glass tubes and put in a water bath. The temperature at which the last tiny part of gel is completely dissolved is defined as the equilibrium temperature T^e, and the corresponding concentration is the equilibrium concentration X^e. To guarantee the accuracy of the measurements, in the neighborhood of the equilibrium temperature, the temperature was increased in steps of 0.2 °C and maintained for 30 min at each step.

II.C. Rheological Study. The rheological properties of the organogel were measured by an advanced rheological expansion system (ARES-LS, Rheometric Scientific). Dynamic temperature ramp tests were carried out to obtain the storage modulus G' (a measure of elasticity) and loss modulus G'' (a measure of viscosity) as functions of time. The solid−gel transition was carried out in-situ between two parallel plates of 25 mm diameter separated by a gap of 0.85 mm. The samples were subjected to a sinusoidal oscillation of frequency 0.1 Hz. Except during the dynamic strain analysis experiments, the strain was controlled to obtain a maximum of 0.05% in the sample.

II.D. Transmission Electron Microscopy (TEM). A piece of gel was deposited on a Formvar/carbon-coated copper grid (200 mesh) and removed after a few minutes to leave only some small patches of the gel on the grids. The nanostructure of the gels was observed with a cryo-TEM (JEOL JEM 2010F). Although cryo-TEM has been used to visualize the structures of hydrogels,[20] such a powerful direct imaging technique has not been widely used in organogel systems. Samples for electron microscopy observation are generally prepared by temperature quenching and subsequent fracture, etching, and metal shadowing steps, which make it difficult to preserve the original fiber structure.[1] Using the cryo-TEM technique, the perturbation on the nanostructure of a fiber network can be minimized.

III. Results and Discussion

III.A. Solubility of GP-1 in ISA. It is generally accepted that supersaturation is the thermodynamic driving force for the gel formation. Therefore, to determine this driving force, solubility data are essential. According to van't Hoff's equation, the solubility of a solute in a given solvent can in principle be described by

$$\ln X^e = -\frac{\Delta H_{diss}}{RT^e} + \frac{\Delta S_{diss}}{R} \quad (1)$$

where X^e is the equilibrium concentration at a certain temperature; ΔH_{diss} and ΔS_{diss} denote the molar dissolution enthalpy and entropy, respectively. The implication of eq 1 is that, within a certain concentration range, $\ln X^e$ can be expressed as a linear function of $1/T^e$. On the other hand, the equilibrium concentration X^e as a function of temperature can be obtained if ΔH_{diss} and ΔS_{diss} are known. The van't Hoff plot for the solubility of GP-1 in ISA is given in Figure 4. A good linear correlation is obtained. The values of ΔH_{diss} and ΔS_{diss} determined from the line are 40.6 kJ·mol^{-1} and 0.90 kJ·mol^{-1}·K^{-1}, respectively.

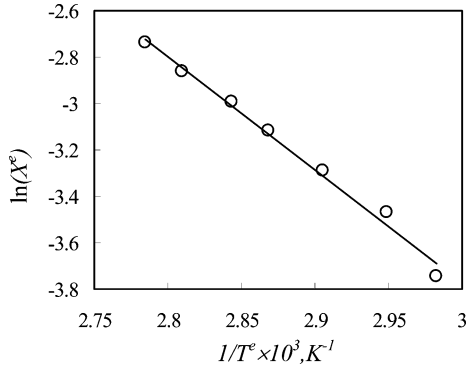

Figure 4. Plot of ln X^e as a function of $1/T^e$.

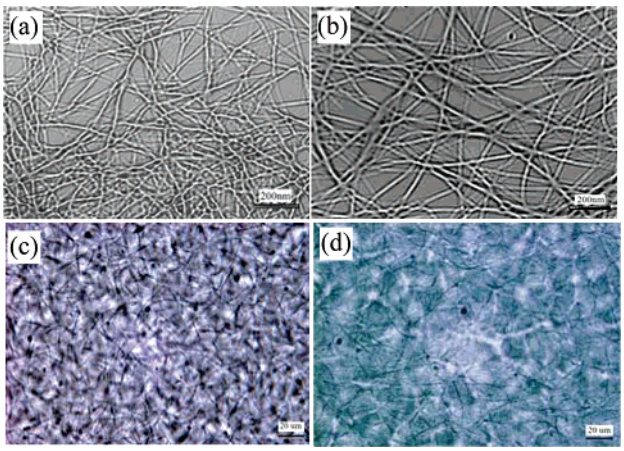

Figure 5. Micro/nanostructure of GP-1 fibrous network formed in ISA. The GP-1 concentration is 4.93 mol %: (a) TEM, 10 °C, scale bar 200 nm; (b) TEM, 30 °C, scale bar 200 nm; (c) microscopy, 30 °C, scale bar 20 μm; (d) microscopy, 35 °C, scale bar 20 μm.

For a certain GP-1 molar fraction X, the supersaturation σ of the system at a certain temperature T can be calculated by

$$\sigma = (X - X^e)/X^e \quad (2)$$

III.B. Micro/Nanostructure of the Fiber Network of GP-1/ISA Gel. Figure 5parts a and b show the TEM images images of the GP-1 fibrous network structure formed at 10 °C and 30 °C, respectively. In ISA, the network of GP-1 is built up by the branching and entanglement of fibers. The microstructure acquired by optical microscope (Figure 5c and d) is similar to that obtained at nanoscale measurements by TEM. This characteristic was also reported for other gel systems.[21−23]

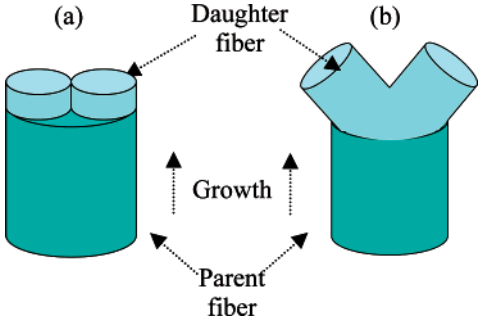

Figure 6. Schematic description of fiber growth and branching: (a) the formation of elongated fibers due to a perfect structural match between the new layer (daughter fiber) and the existing fiber (parent fiber) surface; (b) mismatch nucleation at the surface of fiber tips, leading to crystallographic mismatch branching.

The structure of the GP-1 fiber network in ISA can be well presented by a Cayley tree (cf. Figure 1). For a normal Cayley tree, the branching rate z (number of branches from each branching point) and branching distance ξ (correlation length) are constant parameters during the whole growth. In other words, the end of each branch is the site of growth from which z branches with constant length of ξ grow. The structure, especially the mesh size of the network, is determined by these two parameters. Therefore, by controlling these two parameters, the desired fiber network can be created. This concept is of considerable significance in the creation and design of supramolecular materials.[15]

III.C. Architecture of the Gel Network. It has been verified that the formation of a GP-1 fiber network in ISA was initiated by the primary nucleation of GP-1, followed by subsequent fiber growth and branching.[16] The interconnecting network formation can be regarded as follows: primary nucleation−growth−CMB−growth−CMB ... (cf. Figure 2).

The growth of the fibers in the fibrous axis orientation implies that the crystal structure of the newly created layers matches perfectly with that of the existing surface of fibers (Figure 6a). On the other hand, for any crystallization system, there is a certain probability of mismatch nucleation in which the surface of existing fiber tips serves as a perfect substrate for self- or auto-epitaxial nucleation at relatively high supersaturations (Figure 6b). The occurrence of the mismatch nucleation, leading to the occurrence of new fiber branches, depends on the structural match between the substrate and the nucleating phase and on the supersaturation.[24]

Figure 5 demonstrated that at a lower temperature (higher supersaturation), a network with more densely and uniformly branched fibers can be obtained, while the branching rate z remains unchanged ($z = 2$). The fibers are also thinner at a higher supersaturation. Comparison between structures at the microscale level shown in Figure 5c and d also leads to the same conclusion. The above observation implies that designing the architecture of the fiber network is feasible by manipulating the supersaturation of the system. By varying supersaturation, the rheological properties of the gel can also be tailored.

Figure 7 gives the evolution of the storage modulus G′ at 20 °C and 35 °C. It shows that, after a certain time, which is named the gelation time t_g, G' increases sharply from around zero indicating the initiation of gelation and approaches a constant value G'_{max} upon the completion of the fiber network. Due to the higher supersaturation and more branched network at 20 °C, faster gelation and a higher G'_{max} were obtained. The influence of supersaturation on G'_{max} will be discussed further in section III.D.

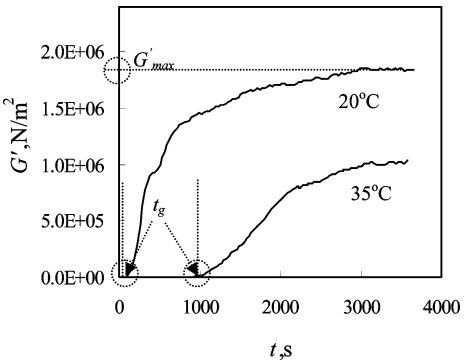

Figure 7. Evolution of the storage modulus G'.

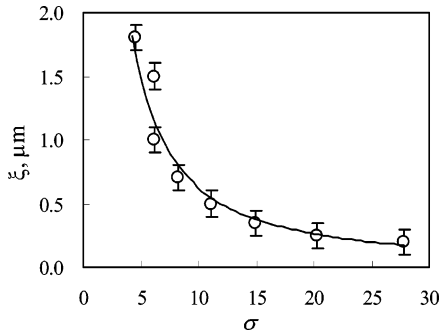

Figure 8. Effect of supersaturation on the correlation length of fiber network.

To get a full picture of the supersaturation-dependence of the network structure, a series of TEM analyses were performed at different supersaturations, which were obtained by fixing the GP-1 concentration at 4.93 mol %, while changing the temperature for gelation. The dependence of correlation length ξ (the distance between two adjacent branching points along one fiber) obtained from TEM images on supersaturation σ is quantified and described in Figure 8. At a low supersaturation, a good structure match occurs between the new layers and the surface of the growing fiber tips.[24]As a result, a fiber network with longer correlation length and larger mesh size can be obtained. On the contrary, a higher supersaturation leads to shorter correlation length and a denser network. The relationship between correlation length ξ and supersaturation σ can be described by the following equation:

$$\xi = 11.07\sigma^{-1.25} \tag{3}$$

Figure 8 also shows that when supersaturation is increased to above a certain level, the correlation length does not show significant change. This could be due to the fact that the crystallization process of fiber formation turns out to be kinetically controlled due to the limited diffusion of gelator molecules, as a result of an increase of the bulk concentration and a high solvent viscosity at very low temperatures. This will reduce the surface supersaturation of GP-1 molecules at the growing fiber tips.

The effects of supersaturation on the structural match can be analyzed as follows.

According to 3D nucleation models, the nucleation rate J, the number of critical nuclei generated per unit time−volume at the substrate can be expressed as[24,25]

$$J = ff^{1/2}B \exp\left[-\frac{16\pi\gamma_{cf}^{3}\Omega^{2}}{3(kT)^{3}(\Delta\mu/kT)^{2}f}\right] \tag{4}$$

$$\text{with } \Delta\mu/kT \cong \ln(X/X^{e}) = \ln(1+\sigma) \tag{5}$$

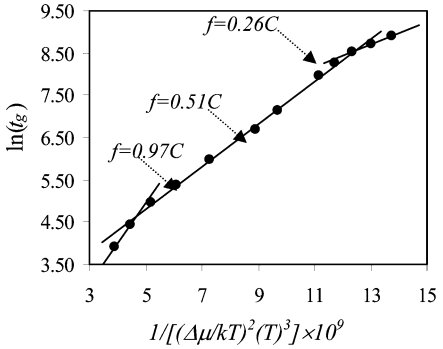

Figure 9. Plot of $\ln(t_g)$ vs $1/[(\Delta\mu/kT)^2T^3]$.

where J is the nucleation rate defined as the number of critical nuclei generated per unit time−volume, B is the kink kinetic coefficient and is constant for a given system, k is Boltzmann's constant, T is temperature, and $\Delta\mu$ denotes the chemical potential difference between GP-1 molecules in the fiber and those in the liquid phase.

If the formation of the fiber network is initiated by nucleation, one should have $t_g \sim 1/J$. Hence, according to eq 4, for such a system, a linear relationship between $ln(t_g)$ and $1/[(\Delta\mu/kT)^2(T)^3]$ can be obtained. The slope of the line corresponds to f. A lower f means that a better structural match exists between the crystalline phase and the fluid phase.

Figure 9 shows the relationship between $\ln(t_g)$ and $1/[(\Delta\mu/kT)^2(T)^3]$. It shows that, depending on the supersaturation of the system, three linear correlations can be identified. It indicates that, by increasing the supersaturation, structural mismatch can be enhanced (f increases with supersaturation; C is a constant), which leads to increased fiber branching in the gel system.

III.D. Engineering the Rheological Properties of the Gel. Rheological properties are the most important properties of a gel system. It is generally accepted that organogels are soft materials that possess both the elasticity of solid (fiber network) and the viscosity of liquid (solvent entrapped in the network). That is, they are viscoelastic in nature. The elastic and viscous properties can be quantified by the storage modulus G' and loss modulus G'', respectively. Figure 7 indicates that the desired macroscopic properties can be obtained through the design of the architecture of its fiber network.

Figure 10a gives the storage modulus of the gel as a function of the supersaturation of the system. It can be seen that, initially, G'_{max} increases quickly with supersaturation, which is attributable to the increasing degree of branching and increasing fiber mass. On the other hand, G'_{max} reaches a constant value at very high concentrations. Correlations between the storage modulus and the supersaturation have been attempted by authors. It has been reported that the variation of G'_{max} with the distance from the equilibrium concentration, $C - C^e$, can be described by a power law expression, $G'_{max} = a(C - C^e)^b$, where a and b are constants; C and C^e are the gelator concentration and its equilibrium concentration at a certain temperature.[26] However, this correlation is not verified within the entire supersaturation range of this gel and other gels we studied. In fact, this linear relationship normally holds in the range of low supersaturations. With an increase of supersaturation, the nucleation rate also increases, resulting in the formation of a larger number of individual networks in a gel system (Figure 2). The entanglements between fibers from different smaller networks are normally weaker, compared with the permanent junctions of fibers in an individual structure unit. Therefore, the increase of the number of structure units with an increase of the nucleation rate reduces the integrity and compromises the overall mechanical strength of the entire network. In addition, at high enough supersaturations, the contribution from structure change is much less significant (Figure 8). A combination of these two aspects could explain the level-off of the curve in Figure 10a. This negative effect arising from the higher nucleation rate at a higher supersaturation is more evident in gel systems with spherulite network structures, where clearer boundaries between individual structure units can be identified.[4]

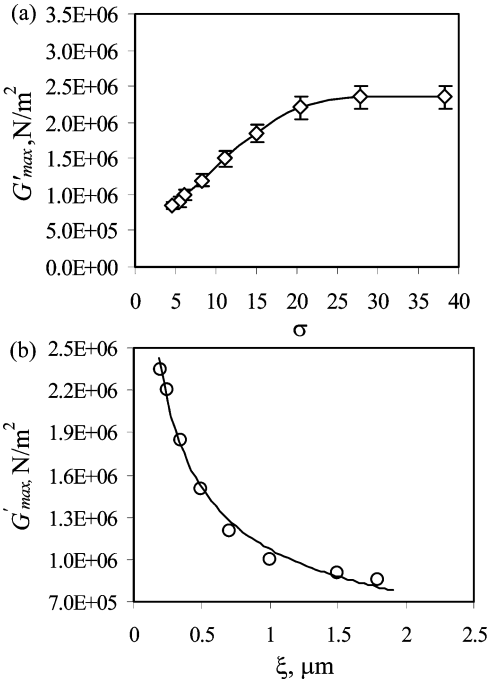

Figure 10. Effects of supersaturation and correlation length on the storage modulus: (a) G'_{max} as a function of supersaturation; (b) G'_{max} as a function of correlation length.

It is worth mentioning that although correlations between storage modulus and supersaturation can provide useful information on the mass-dependence of rheological properties, they are far from being enough to give insight into the structural dependence of such properties. For a gel system, its macroscopic properties are to a great degree determined by the nature of the fiber assembly. In terms of elasticity, it is believed that, for a fixed fiber mass, the number of permanent junctions such as branching points is the dominant factor, while the nonpermanent or transient entanglement between fibers plays a minor role. To demonstrate the contribution of the fiber branching density, G'_{max} is given as a function of correlation length ξ in Figure 10b. It demonstrates that G'_{max} decreases with an increase of ξ. The correlation can be well described by a power law function (eq 6).

$$G'_{max} = 1.07 \times 10^6 \cdot \xi^{-0.49} \tag{6}$$

Equation 6 gives the structure-dependence of the gel elasticity. A more densely branched network results in a gel with better elasticity. Power law correlations between G' and pore size have been proposed for polymer gels and networks. For example, for semiflexible and flexible polymer networks, the exponents are proposed to be -2 and -3, respectively.[27,28] According to the proposed models, the elasticity is also affected by the rigidity of the chains of a network. For small molecule organic gels such as the GP-1/ISA gel of this work, a correlation between G' and ξ has not been proposed or observed empirically, to the best of our knowledge. To verify whether a power law correlation is generally applicable to this type of gel, further

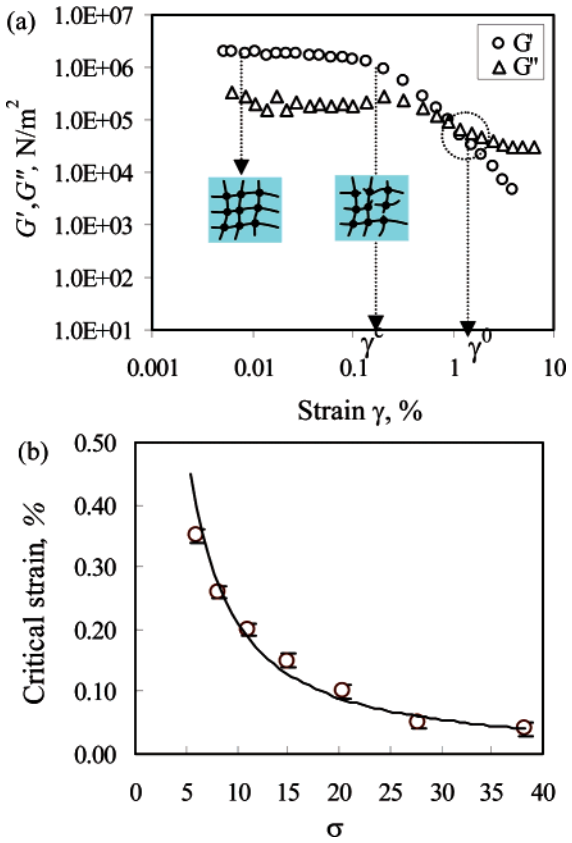

Figure 11. Critical strain of the gel: (a) determination of the critical strain (see text); (b) variation of critical strain γ^c with supersaturation.

work will be done for other gel systems. In addition, theoretical investigation is needed to get a clear understanding of this issue.

Critical strain γ^c is also an important rheological property of a gel, as it is a measure of the brittleness of the fiber network. Figure 11a displays the storage, G', and loss moduli, G'', as a function of strain applied on the gel formed at 20 °C. It shows that at strains lower than ca. 0.15% a linear region exists (strain-independent) and G'' is only about $^1/_{10}$ of G', traits which characterize a good elastic gel. At higher strains, a sharp decrease of G' and G'' is observed, which is attributable to the partial breakdown of the gel network structure. The strain above which a dramatic decrease of G' occurs is named critical strain γ^c. This is a characteristic property of materials with structures containing permanent and strong junctions. Increasing strain further, G' decreases linearly, corresponding to the gradual breaking down of the network structure. When γ reaches a certain level γ^0, most of the structure has been broken down and G' decreases below G''. Beyond this point, the viscous property of the gel is dominant.

Despite the increase of the storage modulus with supersaturation, the relationship between critical strain γ^c and supersaturation shows a reverse trend, as displayed in Figure 11b. This indicates that the network becomes more brittle as the degree of branching increases. Compared with the unbranched fibers, the branching junctions are weaker to withstand the same stretching force. Therefore, the larger the proportion of branching points in a network, the more brittle it is. A good power law correlation between the critical strain and supersaturation was obtained.

$$\gamma^c = 3.59 \cdot \sigma^{-1.23} \qquad (7)$$

IV. Conclusions

The results showed that structure, especially the correlation length of the fiber networks, of the gel formed by *N*-lauroyl-L-glutamic acid di-*n*-butylamide in isostearyl alcohol can be finely tuned by adjusting the supersaturation of the system. The formation and architecture of the 3D interconnecting fiber network in this gel is based on the mechanism of supersaturation-driven crystallographic mismatch branching. The modification in the structure of the fiber network has a direct impact on the macroscopic properties of the gel. The approach in this study has considerable significance in many applications, such as control of the release rate of drug molecules. On the basis of the results of this work and our recent application of this gel in transdermal drug release, our next step is to examine the influence of the thermal architecture of this gel on controlled drug release.

Acknowledgment. The financial support from the Agency for Science, Technology and Research (A*Star) of Singapore (Project No. R-144-000-093-305) is acknowledged. The authors would like to thank Prof. Janaky Narayanan for helpful comments and revision of the text.

References and Notes

(1) Terech, P.; Weiss, R. G. *Chem. Rev.* **1997**, *97*, 3133.
(2) van Esch, J. H.; Feringa, B. L. *Angew. Chem., Int. Ed.* **2000**, *39*, 2263.
(3) Shirakawa, M.; Fujita, N.; Shinkai, S. *J. Am. Chem. Soc.* **2003**, *125*, 9902.
(4) Huang, X.; Terech, P.; Raghavan, S. R.; Weiss, R. G. *J. Am. Chem. Soc.* **2005**, *127*, 4336.
(5) Kishimura, A.; Yamashita, T.; Aida, T. *J. Am. Chem. Soc.* **2005**, *127*, 179.
(6) Pisal, S.; Shelke, V.; Mahadik, K.; Kadam, S. *AAPS PharmSciTech* **2004**, *5* (4), Article No. 63.
(7) Dowling, T. C.; Arjomand, M.; Lin, E. T.; Allen, L. V.; McPherson, M. L. *Am. J. Health-Syst. Pharm.* **2004**, *61*, 2541.
(8) Kang, L.; Liu, X. Y.; Sawant, P. D.; Ho, P. C.; Chan, Y. W.; Chan, S. Y. *J. Controlled Release* **2005**, *106*, 88.
(9) Love, C. S.; Chechik, V.; Smith, D. K.; Wilson, K.; Ashworth, I.; Brennan, C. *Chem. Commun.* **2005**, *15*, 1971.
(10) Jung, J. H.; Kobayashi, H.; Masuda, M.; Shimizu, T.; Shinkai, S. *J. Am. Chem. Soc.* **2001**, *123*, 8785.
(11) Kishida, T.; Fujita, N.; Sada, K.; Shinkai, S. *J. Am. Chem. Soc.* **2005**, *127*, 7298.
(12) Oya, T.; Enoki, T.; Grosberg, A. Y.; Masamune, S.; Sakiyama, T.; Takeoka, Y.; Tanaka, K.; Wang, G. Q.; Yilmaz, Y.; Feld, M. S.; Dasari, R.; Tanaka, T. *Science* **1999**, *286*, 1543.
(13) Corriu, R. J. P.; Leclercq, D. *Angew. Chem., Int. Ed. Engl.* **1996**, *35*, 1420.
(14) Gronwald, O.; Snip, E.; Shinkai, S. *Curr. Opin. Colloid Interface Sci.* **2002**, *7*, 148.
(15) Liu, X. Y.; Sawant, P. D.; Tan, W. B.; Noor, I. B. M.; Pramesti, C.; Chen, B. H. *J. Am. Chem. Soc.* **2002**, *124*, 15055.
(16) Liu, X. Y.; Sawant, P. D. *Adv. Mater.* **2002**, *14*, 421.
(17) Liu, X. Y.; Sawant, P. D. *Angew. Chem., Int. Ed.* **2002**, *41*, 3641.
(18) Schwartzmiller, D. H.; Randen, N. A. U.S. Patent 6,200,596, Appl. No. 186216, March 13, 2001.
(19) Gagnebien, D.; Simon, P. U.S. Patent 6,150,422, Appl. No. 815428, March 11, 1997.
(20) Hartgerink, J. D.; Beniash, E.; Stupp, S. I. *Science* **2001**, *294*, 1684; Estroff, L. A.; Leiserowitz, L.; Addadi, L.; Weiner, S.; Hamilton, A. D. *Adv. Mater.* **2003**, *15*, 38.
(21) Beginn, U.; Keinath, S.; Moller, M. *Macromol. Chem. Phys.* **1998**, *199*, 2379.
(22) Ballabh, A.; Trivedi, D. R.; Dastidar, P. *Chem. Mater.* **2003**, *15*, 2136.
(23) An, B. K.; Lee, D. S.; Lee, J. S.; Park, Y. S.; Song, H. S.; Park, S. Y. *J. Am. Chem. Soc.* **2004**, *126*, 10232.
(24) Strom, C. S.; Liu, X. Y.; Wang, M. *J. Phys. Chem. B* **2000**, *104*, 9638; Liu, X. Y. *J. Chem. Phys.* **2000**, *112*, 9949.
(25) Chernov, A. A. *Modern Crystallography III—Crystal Growth*; Springer: Berlin, 1984.
(26) Brinksma, J.; Feringa, B. L.; Kellogg, R. M.; Vreeker, R.; van Esch, J. *Langmuir* **2000**, *16*, 9249.
(27) MacKintosh, F. C.; Kas, J.; Janmey, P. A. *Phys. Rev. Lett.* **1995**, *75*, 4425; Shin, J. H.; Gardel, M. L.; Mahadevan, L.; Matsudaira, P.; Weitz, D. A. *Proc. Natl. Acad. Sci. U. S. A.* **2004**, *101*, 9636.
(28) de Gennes, P. G. *Scaling Concepts in Polymers Physics*; Cornell: Ithaca, NY, 1979.